Materials Science in Semiconductor Processing 135 (2021) 106076

Contents lists available at ScienceDirect

Materials Science in Semiconductor Processing

journal homepage: www.elsevier.com/locate/mssp

Full length article

Influence of position dependent effective mass on impurity binding energy and absorption in quantum wells with the Konwent potential

E.B. Al [a], E. Kasapoglu [a,*], S. Sakiroglu [b], H. Sari [c], I. Sökmen [b]

[a] Sivas Cumhuriyet University, Faculty of Science, Physics Department, 58140 Sivas, Turkey
[b] Dokuz Eylul University, Faculty of Science, Physics Department, 35390 Izmir, Turkey
[c] Sivas Cumhuriyet University, Faculty of Education, Department of Mathematical and Natural Science Education, 58140 Sivas, Turkey

ARTICLE INFO

Keywords:
Position-dependent effective mass
Konwent potential
Impurity

ABSTRACT

In this work, we perform a theoretical investigation on the effect of position-dependent effective mass on binding energy and optical absorption coefficient for donor impurities in single and double quantum wells defined by Konwent potential. We have used the diagonalization method by choosing a wave function based on the trigonometric orthonormal base functions that are solutions of an infinite square quantum well to get the energy spectrum of the system, the variational method for impurity binding energy is used and also linear absorption coefficient is deduced from the density matrix approach and perturbation expansion method. Numerical results reveal that impurity binding energy as well as the linear optical absorption coefficient are remarkably affected by the confinement potential parameters, position of an impurity and the approach used for the effective electron mass. Moreover, it is seen that with an appropriate choice of the structure parameters and position dependence effective mass distribution, the optical response of the system can be tailored in a controllable manner.

1. Introduction

Rapid development in nanotechnology has enabled the growth of low dimensional systems with intriguing electronic and optical properties. These structures are focus of special and increasing attention due to their extensive application area in optoelectronic device technology [1–6]. Tunability of the physical properties to fulfill the practical needs can be realized by a proper choice of structure geometry, material parameters and in a cost-effective way by using the external agents as electric, magnetic and laser fields [7–10]. Progress in material growth techniques render possible the growth of quantum wells (QWs) with varying confinement potentials being symmetric or asymmetric with respect to well center. Interaction potentials as Gaussian, Morse, Tietz–Hua, Razavy, Mathieu etc. are widely used in material physics for specifying the realistic confinement of charge carriers [11–16]. In this context Konwent potential stands as an interesting function for representing the confinement effect in QW with ductile geometry [17–19]. Besides it is well known that the presence of impurity states affects remarkably the electrical and optical characteristics of nanomaterials that are more pronounced than their bulk counterparts [20]. Therefore, it is significant to figure out deeply the impurity-related effects on the semiconductor nanostructures in order to control the performance of optoelectronic devices. The concept of position-dependent electronic effective mass (PDM) is relying on spatial variation of electron effective mass in layered heterostructures [21–25]. Along with the knowledge that the effective mass of charge carriers differs close to the interlayer surface of multilayered heterostructures, appropriate theory for the electronic and optical characteristics of low dimensional systems can be established with a convenient model for potential profile and considering the PDM-effect [26,27]. Intensive research has been carried out for better understanding of the physical properties of QW with impurity by considering the PDM effect [28–30]. The effects of spatially dependent effective mass on the optical properties in parabolic quantum wells have been examined by Herling and Rustagi [31]. The donor ionization energies in different quantum structures under the effects of the constant effective mass and position dependent effective mass have been reported in Ref. [20]. Panahi et al. studied the binding energy in QW under magnetic field by taking into account the spatially varying effective mass effects [32]. Classical particle in 1D and 2D harmonic potential has been discussed by Khlevniuk and coworkers [33]. Intersubband optical transitions and bound energy states in QW defined with Tietz–Hua potential considering PDM has been analyzed by Sari et al. [13]. Ovando et al. [34] studied the solution of position-dependent mass Schrödinger equation with Morse potential. Researches on spatially varying effective mass in low-dimensional

* Corresponding author.
E-mail address: ekasap@cumhuriyet.edu.tr (E. Kasapoglu).

https://doi.org/10.1016/j.mssp.2021.106076
Received 26 March 2021; Received in revised form 4 June 2021; Accepted 29 June 2021
Available online 13 July 2021

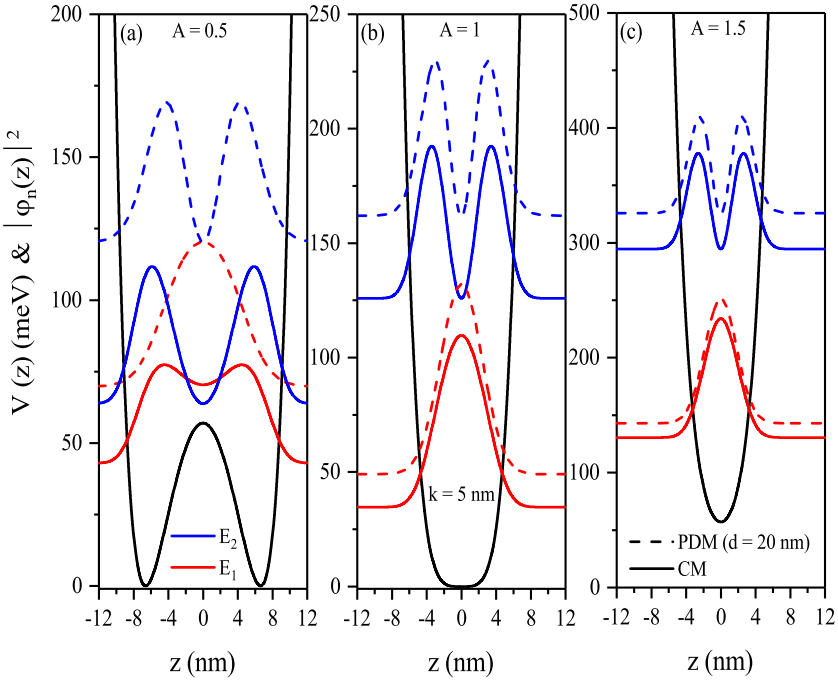

Fig. 1. The confinement potential profiles and probability density distributions for ground-1s and first excited-2s states of the electron confined in the QWs with Konwent potential for a constant mass (CM) and PDM versus the position. Results are for: (a) $A = 0.5$, (b) $A = 1$, and (c) $A = 1.5$.

structures reveal its significant effects on the electronic spectrum and optical characteristics [32].

In this work, we aim to exhibit the effect of spatially varying effective mass on impurity binding energy and optical absorption in quantum wells represented with the Konwent potential. Variational approach is utilized for the calculation of energy eigenvalues and eigenstates and linear optical absorption coefficient is deduced from the density matrix formalism. The organization of the paper is as follows: Section 2 consists of theoretical framework. Section 3 is devoted to the obtained results and a brief conclusion is presented in Section 4.

2. Theory

Within the framework of the effective mass approximation, Hamiltonian for an electron and donor impurity system is given by [14,21],

$$H = -\vec{\nabla}\frac{\hbar^2}{2m(z)}\cdot\vec{\nabla} - \frac{e^2}{\epsilon r} + V_{KP}(z), \tag{1}$$

where $m(z)$ is the position dependent effective mass of the electron, ϵ is the static dielectric constant of the semiconductor material, $r = \sqrt{\rho^2 + (z - z_i^2)}$ is distance between electron and donor impurity center ($\rho = \sqrt{x^2 + y^2}$). Additionally, z and z_i are the electron and impurity coordinates along the z-axis, and $V_{KP}(z)$ is the Konwent confinement potential and its functional form is given as follows [17]:

$$V_{KP}(z) = V_0\left(A\cosh\left(\frac{z}{k}\right) - 1\right)^2, \tag{2}$$

where V_0 is potential parameter, k-parameter is related to the well width and A-parameter is a positive constant. Depending on the choice of A-parameter, shape of the potential becomes single or double quantum well. As seen Figs. 1 (a-c), potential is double QW for the values of $A < 1$, for $A = 1$, the structure is in the form of a broad single quantum well (QW) which has the flat bottom, and for $A > 1$, potential becomes a single parabolic QW that bottom shifts toward higher energy values. If desired, parameter-A can be selected as negative, but double-well potential is not observed.

The position dependent mass distribution is chosen as follows [13],

$$m(z) = m^* sech^2\left(\frac{\pi z}{d}\right), \tag{3}$$

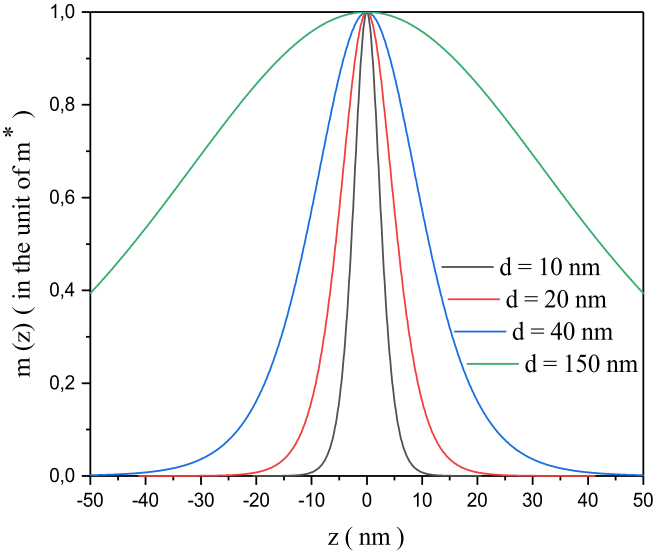

Fig. 2. The position dependent effective mass distribution as a function of the z-position for different values of d-parameter.

where d-parameter describes the effective length of PDM distribution, and $m^* = 0.067m_0$ is the effective mass at $z = 0$ (the bulk material effective mass, with m_0-the free electron mass). PDM distribution as a function of the z-position for different values of d-parameter that describes the effective length of the PDM distribution is given in Fig. 2. As d-value grows up, $m(z)$ approaches to the value of electron mass in the bulk material of interest and also as d-parameter gets to be large the uniform behavior, stability and the spatially extension of the effective mass increase as seen in this figure. This effective mass distribution is suitable to represent a solitonic profile found in condensed matter and low energy nuclear physics [35,36].

The one-dimensional time-independent Schrödinger equation for an electron with a PDM can be expressed as

$$\left[-\frac{d}{dz}\frac{\hbar^2}{2m(z)}\frac{d}{dz}+V_{KP}(z)\right]\varphi(z)=E_z\varphi(z). \tag{4}$$

To solve this equation, we used the diagonalization method by choosing orthonormal base functions that are solutions of an infinite square quantum well with L-width. L is infinite well width at the far end of QW which is large enough when comparing with the single and double quantum well widths with the Konwent potential. The L-value is determined according to the convergence of the energy eigenvalues.

The bases are formed as

$$\varphi_n(z)=\sqrt{\frac{2}{L}}\cos\left[\frac{n\pi}{L}z-\delta_n\right], \tag{5}$$

where

$$\delta_n=\begin{cases}0, & n\ is\ odd\\ \frac{\pi}{2}, & n\ is\ even\end{cases}, \tag{6}$$

and so, the wave function in the z-direction is expanded in a set of basis function as follows

$$\varphi(z)=\sum_{n=1}^{N}c_n\varphi_n(z), \tag{7}$$

where N is the size of the matrix. When calculating the wave function $\varphi(z)$, we ensured that the E_z eigenvalues are independent of chosen infinite potential well width-L, and the wave functions are localized in the well region. This method requires embedding any well potential into an infinite square well, whose presence of the confining walls have no effect on the solutions. The width of the infinite square well has been chosen large enough so that the solutions are not sensitive to infinite walls. Further, the size of the matrix (the upper limit-N of the sum in Eq. (7)) is increased until convergence to any desired accuracy is achieved. It should be noted that in this study, the value of N is chosen large enough to guarantee a precise accuracy also for all confined states in different types of quantum wells considered.

The energies of the $1s$ and $2s$ impurity states are calculated through a variational approach. For each state, the total wavefunction-$\psi(r,\lambda)$ is as follows

$$\psi(r,\lambda)=\varphi(z)\chi(r,\lambda), \tag{8}$$

where $\chi(r,\lambda)$ are the hydrogenic wave functions and for $1s$ and $2s$ impurity states they are given as follows [37]

$$\chi_{1s}(r,\lambda_1)=N_1e^{-\frac{r}{\lambda_1}}, \tag{9}$$

$$\chi_{2s}(r,\lambda_2)=N_2\left(2-\frac{r}{\lambda_2}\right)e^{-\frac{r}{2\lambda_2}}, \tag{10}$$

respectively, where N_1 and N_2 are the normalization constants, λ_1 and λ_2 are the variational parameters.

The binding energy of the ground and first excited impurity states is given by

$$E_b^{1s,2s}=E_z^{1,2}-\min_{\lambda_1,\lambda_2}\langle\psi|H|\psi\rangle, \tag{11}$$

where, $E_z^{1,2}$ is the ground or first excited state energies of electron in the QW with the Konwent potential (E_z^1 (E_z^2) is used for the binding energy of $1s$ ($2s$) state) and second term gives the impurity energies (E^{1s} and E^{2s}) which are found by minimizing the expectation value of the Hamiltonian of electron confined within the QW with the Konwent potential according to the variational parameters (λ_1 and λ_2).

By employing the density matrix formalism and the perturbation expansion method, the linear AC for the transitions between any two impurity states is obtained as follows [38,39],

$$\alpha^{(1)}(\omega)=\sqrt{\frac{\mu_0}{\varepsilon_r}}\frac{\sigma_s\Gamma_{ij}}{(E_{ij}-\hbar\omega)^2+(\hbar\Gamma_{ij})^2}\hbar\omega|M_{ij}|^2, \tag{12}$$

where, $\varepsilon_r=n_r^2\varepsilon_0$ is the real part of the permittivity, σ_s is the carrier density in the system, μ_0 is the vacuum permeability, $E_{ij}=E_j-E_i$ is the transition energy between any two impurity states, $M_{ij}=\langle\Psi_i|ez|\Psi_j\rangle$ is the dipole matrix element for transition between the eigenstates Ψ_i and Ψ_j for z-polarization of the incident radiation and Γ_{ij}-the relaxation rate which is equals to the inverse relaxation time T_{ij}.

Since the structures under consideration are symmetrical and they are not exposed to any external factors, the nonlinear effect is quite small. Therefore, only the linear AC is investigated in the study. Further, although the dipole matrix element seems to be the dominant parameter on the amplitude of the linear AC, it is not sufficient by itself to explain the amplitude changes. For this reason, the term $\Omega=e^{-2}\hbar\omega|M_{ij}|^2$ is used to explain the amplitude changes of the linear AC in Eq. (12) according to the parameter values considered.

3. Results and discussion

In this section we present the numerical results for impurity binding energies and intersubband optical transitions in Konwent QW influenced by the PDM. Parameters, commonly used for typical GaAs/GaAlAs materials, are chosen as follows: $\epsilon=12.58$, $V_0=228$ meV, $n_r=3.2$, $T_{ij}=0.4$ ps, $\Gamma_{ij}=1/T_{ij}$, $\mu=4\pi\times10^{-7}$ H/m, $\sigma_s=3\times10^{22}$ m^{-3}.

Before discussing the effect of PDM on the linear optical absorption coefficient, it would be important to examine the general behavior of potential profile of QW grown along the z-axis. Figs. 1 (a-c) show the Konwent confinement potentials for different values of parameter A, the probability density distributions corresponding to energies of the ground and first excited states versus the z-coordinate. Solid (dashed) lines correspond to the results under CM (PDM) approximation while the red (blue) color indicates the ground state-$1s$ (first excited state-$2s$). The A-parameter identifying prominently the shape of the potential is chosen as 0.5, 1 and 1.5. In case of $A<1$ double QW is formed whereas for $A\geq1$ the potential turns into a single well. Further increase in the A-parameter causes a shift of the potential bottom toward higher energy values and consequently the energies corresponding to $1s$ and $2s$ states becomes greater with inclusion of spatially varying effective mass. The important point that stand out is that the effect of PDM is more evident for systems with a weaker localization of electron.

Figs. 3 (a-b) depict the variation of impurity binding energies of $1s$ and $2s$ state as a function of impurity position for three values of A and $k=5$ nm. Results for CM and PDM approach are shown with solid and dashed lines, respectively.

We see that the greatest binding energy for $1s$-state is obtained for on-center impurity case and $A=1.5$ while binding energy decreases smoothly for impurity locating far away the center of the well. We should note that at sufficiently strong confinements binding energy approaches to those of CM case. On the other hand, presented results reveal that QW potential with $A=0.5$ parameter is more sensitive to the used approach for effective electron mass especially for impurities in the vicinity of the QW center. z_i-dependence of the binding energy for the first excited state shows a symmetric behavior with respect to $z_i=0$ with the smallest value at well center. As known, the binding energy increases or decreases due to the distance between the localization of the electron confined in the QWs and the impurity position. This behavior is a consequence of the enhancement/reduction in the overlap of the electron-donor impurity wave functions owing to the strengthening/weakening of the Coulombic interaction between the electron and donor impurity.

Fig. 4 compares the binding energy values of the ground and first excited states for CM and PDM cases versus the k-parameter considering different values of d-parameter related with the effective length of PDM distribution. We set impurity location at $z_i=0$ and consider three values for A.

The figure demonstrates that augmentation in the k-parameter results with a decrease in binding energy for the chosen parameters set expect $d=10$ nm case of PDM. Distinction between binding energies for

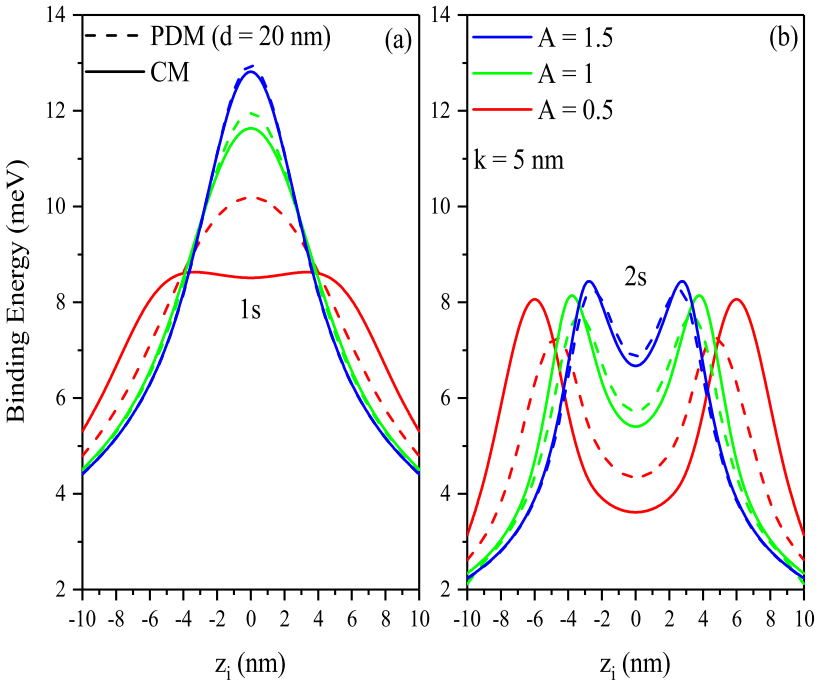

Fig. 3. Impurity binding energies of 1*s* and 2*s* states versus the impurity position for all *A*-values under consideration and for $k = 5$ nm. Results are for CM (solid lines) and PDM (dashed lines).

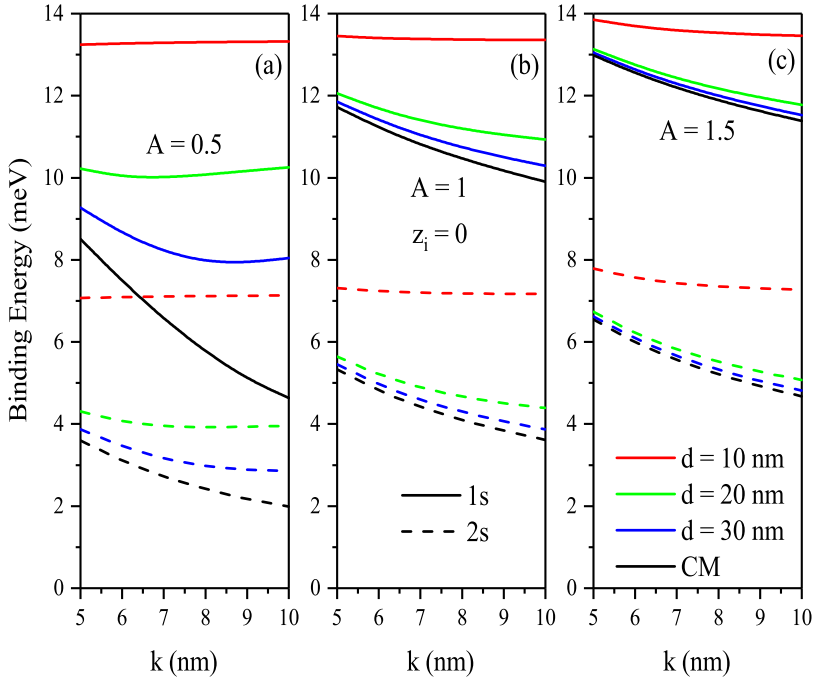

Fig. 4. Binding energies of 1*s* and 2*s* states as a function of *k*-parameter for on-center donor impurity and for different *d* values: (a) $A = 0.5$, (b) $A = 1$, and (c) $A = 1.5$.

different values of *d*-parameter ascends with an increase of *k*-parameter value which is in charge of an extension in the effective well width. As expected, binding energies of both considered eigenstates in single QW structures ($A = 1.5$ and $A = 1.0$) lying at higher energy values than $A = 0.5$ are less affected by choice of *d*-parameter. On contrary, in double QW structure corresponding to $A = 0.5$ a remarkable discrepancy between the cases of CM and PDM is clearly evident. According to above findings it can be inferred that with the reduction in the effective QW width, influence of the spatially dependent mass distribution becomes ineffective. This is a consequence of the increased stability and uniformity of the mass distribution for greater *d*-parameters.

Variation of the linear optical AC versus photon energy for three values of *A*, considering CM and PDM cases for effective mass, is given in Fig. 5(a). Constant potential parameter *k* is set to 5 nm and PDM for $d = 20$ nm is chosen for QW with an on-center impurity. Transition energy and Ω, playing a significant role on the optical coefficients, are exhibited in Fig. 5(b) as a function of *A*-parameter.

From these figures, it is seen that the resonant peak of absorption coefficient considering spatially varying mass case is blue-shifted in

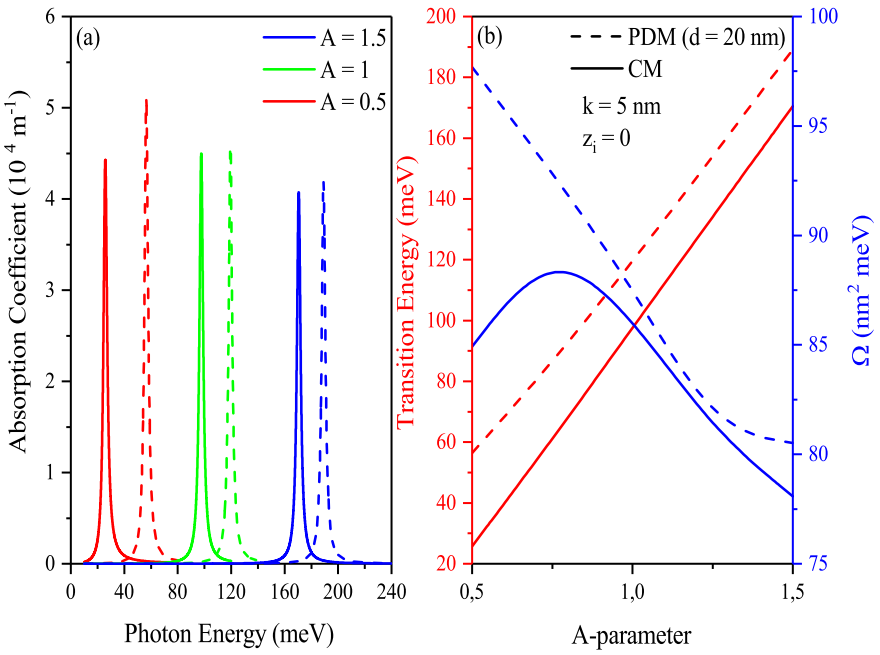

Fig. 5. For on-center impurity and $k = 5$ nm: The variation of the linear AC as a function of the photon energy for three A-values (a) and the variations of transition energy and Ω-parameter as a function of A-parameter (b). Results are for CM (solid lines) and PDM (dashed lines).

comparison to CM results for all undertaken A-parameters in accordance with the variation of the transition energy shown in Fig. 5(b). Moreover, the resonant peak of the optical AC for single QW systems appears at higher photon energy region because of the enhancement of the confinement potential. Change in the amplitude of resonant peak is notable in double QW structure which exposes the increment in the overlap among wave functions in compliance with the variation of Ω. Besides we see that the transition energy increases linearly for stronger A-parameter with higher values in case of PDM while Ω is not a monotonous function with respect to A especially for CM case.

Figs. 6(a-b) display the impact of increased k-value (in comparison with Fig. 5) on the linear optical AC as a function of incident photon energy, and the dependence of the transition energy and Ω versus the A-parameter, respectively.

As seen from Fig. 6(a), increase in the k-value causes a remarkable red-shift in the position of the resonant peaks of AC which relies on the fact that the effective range of confinement potential gets to be larger. Also a rise in the peak amplitudes of the AC relative to $k = 5$ nm case in both approaches for spatially dependent effective electron mass distributions is visible, except $A = 0.5$. In addition, strengthening in A-parameter leads to the observation of resonant AC peaks at higher photon energy regions. On the other hand, taking into account of PDM causes a shift in the peak positions of AC toward higher energies more apparent for a system with $A = 0.5$, in consistency with the variation of the transition energy seen in Fig. 6(b). Moreover tuning the system toward double QW case eventuate with augmentation in the resonant peak magnitudes. We should note that the transition energy and Ω shows salient variation for the smallest A-parameter considering PDM and CM cases both for $k = 5$ nm and $k = 10$ nm. This fact can be interpreted as that the influence of PDM becomes more significant in cases of weaker confinement situations.

In order to clarify the effect of d-parameter of spatially varying effective mass distribution on the system characteristics under debate, in Figs. 7(a-b) we present the linear AC versus incident photon energy for three values of A and the variations of transition energy and Ω-parameter as a function of d. We consider the well parameter k of 5 nm and on-center impurity case.

The main feature seen from Fig. 7(a) is that the reduction in d-parameter give cause for a shift of the resonance peak of AC toward higher energies compared to the CM case and assisted with an increase in its magnitude (except $d = 10$ nm) which is more pronounced for $A = 0.5$. Fig. 7(b) evinces that the transition energies are higher for stronger A-values and diminish with an increase in the d-parameter particularly clear for double QW system. It also should be noted that the distinction between the transition energies for three A-parameters becomes more apparent at spatially varying mass distribution for $d = 30$ nm. Additionally this figure depicts the variation of Ω: for a single QW with strong confinement, Ω is almost unaffected by d, while for $A = 1$ and $A = 0.5$ it is a nonmonotonic function of d and an abrupt change is observed around PDM of $d = 20$ nm. One may notice that for narrow PDM distribution (corresponding to smaller d-values), the effective mass between the central region of QW and the interface with the potential barrier is distinctive. Under this situation, the presence of the potential barriers is perceived more intensively by the charge carriers.

4. Conclusions

In this research, we have investigated the impurity binding energy and linear optical absorption coefficient for intersubband transitions between the two-lower lying electronic energy levels of quantum wells defined with Konwent potential by focusing on the effect of PDM. Dependence of the impurity-related electronic structure and optical coefficients is studied for several values of the potential parameters and spatially varying electronic effective mass. The achieved results show that the reduction in impurity binding for higher k-values becomes more apparent in case of smallest A-parameter of Konwent potential which causes an altering of well profile. Besides, taking up the influence of PDM brings about a blue-shift in the position of resonant peak of AC while the alteration in the peak amplitude is clear for $A = 0.5$ on account of the weakening of confinement. Increment in the d-parameter, which causes a broadening of the effective mass distribution, leads to a diminish of the energy interval accompanied with a red-shift of the linear absorption coefficient. The attitude of the optical absorption coefficient is mainly designated by the nonmonotonic behavior of Ω being more pronounced for quantum wells defined with $A = 0.5$ and $A = 1$ parameters. In summary, results are evincing the noteworthy

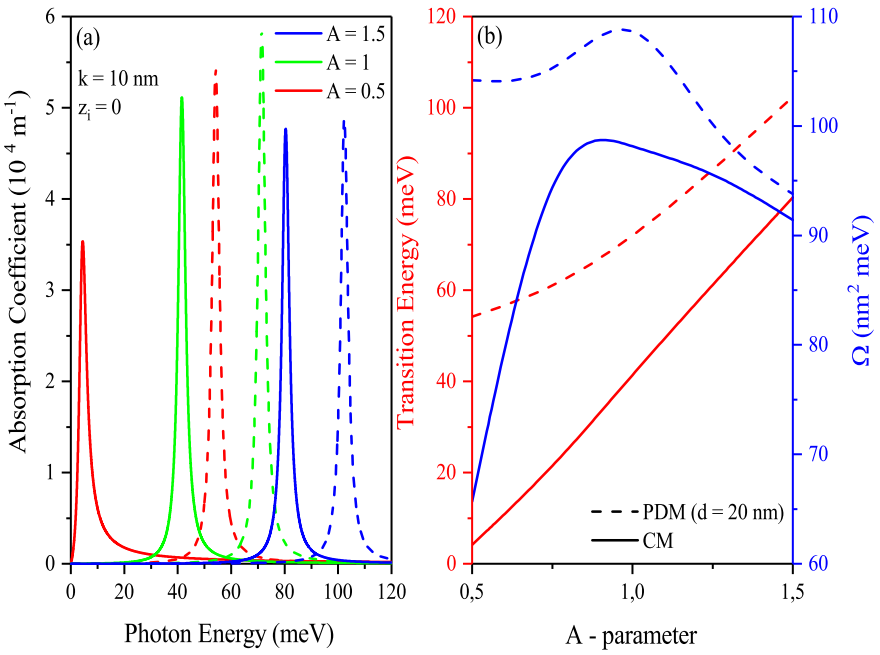

Fig. 6. For on-center impurity and $k = 10$ nm: The variation of the linear AC as a function of the photon energy for three A-values (a) and the variations of transition energy and Ω-parameter as a function of A-parameter (b). Results are for CM (solid lines) and PDM (dashed lines).

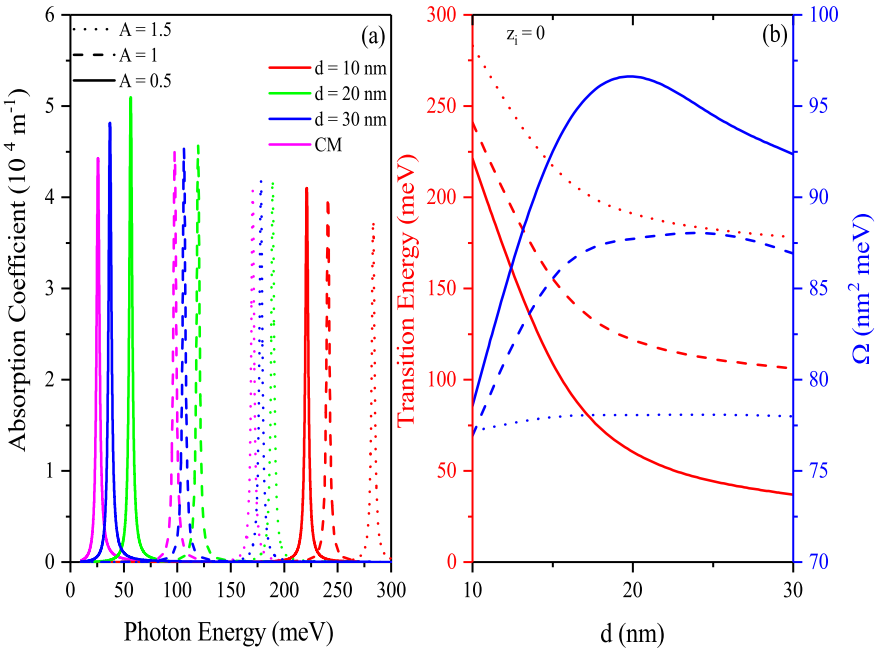

Fig. 7. For on-center impurity and $k = 5$ nm: The variation of the linear AC as a function of the photon energy for different values of parameters A and d (a) and the variations of transition energy and Ω-parameter as a function of d-parameter (b).

change in the impurity binding energy and optical absorption coefficient with respect to the A-parameter of the Konwent potential and d-parameter of the effective mass distribution. Changing the A parameter of the Konwent potential allows us to obtain different structures, among which we can cite single and double quantum wells, whose widths can be changed in a controlled way. Thus, our results show that the electronic and therefore optical properties of the structures we focus on can be adjustable to obtain a convenient response to certain studies or goals by changing the structure parameters. Furthermore, in some values of the A-parameter, Konwent potential is related to the Razavy potential [14] which we have studied before. And our results obtained for this potential related to energies are good agreement with the results of the QWs with Razavy potential.

CRediT authorship contribution statement

E.B. Al: Responsible of the numerical calculations and figures. **E. Kasapoglu:** Proposed the problem, Responsible of the numerical calculations, Writing and editing of the manuscript. **S. Sakiroglu:** Responsible from the writing and editing of manuscript. **H. Sari:** Responsible of the optical properties discussion. **I. Sökmen:** Responsible of the electronic structure discussion.

Declaration of competing interest

The authors declare that they have no known competing financial interests or personal relationships that could have appeared to influence the work reported in this paper.

Data availability statement

All the files with tables, figures, and codes are available. The corresponding author will provide all the files in case they are requested.

References

[1] N.K. Datta, M. Ghosh, Curr. Appl. Phys. 11 (2011) 1222–1227.
[2] H.S. Brandi, A. Latge, L.E. Oliveira, Phys. Rev. B 70 (2004) 153303.
[3] D. Laroze, M. Barseghyan, A. Radu, A.A. Kirakosyan, Phys. B 501 (2016) 1–4.
[4] E.C. Niculescu, Opt. Mater. 64 (2017) 540–547.
[5] J. Ganguly, S. Saha, A. Bera, M. Ghosh, Opt. Commun. 387 (2017) 166–173.
[6] W. Wang, B. Van Duppen, F.M. Peeters, Phys. Rev. B 99 (2019) 014114.
[7] A. Radu, Superlattices Microstruct. 48 (2010) 114–125.
[8] E.C. Niculescu, N. Eseanu, Eur. Phys. J. B 79 (2011) 313–319.
[9] R.L. Restrepo, A.L. Morales, V. Akimov, V. Tulupenko, E. Kasapoglu, F. Ungan, C.A. Duque, Superlattices Microstruct. 87 (2015) 143–148.
[10] R.L. Restrepo, L.F.Castano-Vanegas, J.C. Martinez-Orozco, A.L. Morales, C.A. Duque, Appl. Phys. A 125 (2019) 31.
[11] R. Khordad, S. Goudarzi, H. Bahramiyan, Indian J. Phys. 90 (2016) 659–664.
[12] S. Mo, K. Guo, G. Liu, X. He, J. Lan, Z. Zhou, Thin Solid Films 710 (2020) 138286.
[13] H. Sari, E. Kasapoglu, S. Sakiroglu, I. Sökmen, Optik 178 (2019) 1280–1284.
[14] E. Kasapoglu, H. Sari, I. Sökmen, J.A. Vinasco, D. Laroze, C.A. Duque, Physica E 126 (2021) 114461.
[15] G.-H. Sun, C.-Y. Chen, H. Taud, C. Yánez-Márquez, S.-H. Dong, Phys. Lett. A 384 (2020) 126480.
[16] A.E. Sitnitsky, J. Mol. Spectrosc. 372 (2020) 111347.
[17] H. Konwent, Phys. Lett. A 118 (1986) 467–470.
[18] H. Konwent, P. Machnikowski, P. Magnuszewski, A. Radosz, J. Phys. A: Math. Gen. 31 (1998) 7541–7559.
[19] Q. Dong, S.-S. Dong, E. Hernández-Márquez, R. Silva-Ortigoza, G.-H. Sun, S.-H. Dong, Commun. Theor. Phys. 71 (2019) 231–236.
[20] S. Rajashabala, K. Navaneethakrishnan, Modern Phys. Lett. B 24 (2006) 1529–1541.
[21] X.-H. Qi, X.-J. Kong, J.-J. Liu, Phys. Rev. B 58 (1998) 10578–105582.
[22] A. John Peter, Internat. J. Modern Phys. B 23 (2009) 5109–5118.
[23] M.S. Cunha, H.R. Christiansen, Commun. Theor. Phys. 60 (2013) 642–650.
[24] N. Amir, S. Iqbal, Commun. Theor. Phys. 62 (2014) 790–794.
[25] A. Sebawe Abdalla, H. Eleuch, AIP Adv. 6 (2016) 055011.
[26] H. Sari, E. Kasapoglu, S. Sakiroglu, I. Sökmen, C.A. Duque, Phys. Stat. Sol. B 256 (2019) 1800758.
[27] H. Hassanabadi, W. Sang Chung, S. Zare, M. Alimohammadi, Eur. Phys. J. Plus 132 (2017) 135.
[28] R. Pérez-Alvarez, J.L. Parra-Santiago, P. Pajón-Suárez, Phys. Stat. Sol. B 144 (1987) 639–644.
[29] A. Keshavarz, N. Zamani, J. Comput. Theor. Nanosci. 10 (2013) 2155–2160.
[30] Q. Yu, K. Guo, M. Hu, Z. Zhang, K. Li, D. Liu, J. Phys. Chem. Solids 119 (2018) 50–55.
[31] G.H. Herling, M.L. Rustagi, J. Appl. Phys. 71 (1992) 796–799.
[32] H. Panahi, S. Golshani, M. Doostdar, Phys. B 418 (2013) 47–51.
[33] A. Khlevniuk, V. Tymchyshyn, J. Math. Phys. 59 (2018) 082901.
[34] G. Ovando, J.J. Peña, J. Morales, J. López-Bonilla, J. Phys.: Conf. Ser. 792 (2017) 012037.
[35] H.R. Christiansen, M.S. Cunha, J. Math. Phys. 54 (2013) 122108.
[36] S. Guo-Hua, D. Popov, O. Camacho-Nieto, D. Shi-Hai, Chin. Phys. B 24 (2015) 100303.
[37] E. Kasapoglu, S. Sakiroglu, H. Sari, I. Sokmen, C.A. Duque, Optik 181 (2019) 432–439.
[38] I. Karabulut, S. Baskoutas, J. Appl. Phys. 103 (2008) 073512.
[39] Y. Yakar, B. Cakar, A. Özmen, Opt. Commun. 283 (2010) 1795–1800.